Int. J. Nonlinear Anal. Appl. In Press, 1–12
ISSN: 2008-6822 (electronic)
http://dx.doi.org/10.22075/ijnaa.2025.38344.5508

Utilizing generalized optimality criteria method for optimal structural design under design-dependent pressure loads

Saeed Abedini, Ali Ghoddosian*

Faculty of Mechanical Engineering, Semnan University, Semnan, Iran

(Communicated by Zakieh Avazzadeh)

Abstract

This paper presents a topology optimization framework for continuum structures subjected to design-dependent pressure loads (DDPLs). Unlike fixed external loads, DDPLs change in location, magnitude, and direction as the structural layout evolves, introducing significant challenges in load modeling and numerical stability. To address this issue, the Boundary Identification–Load Evolution (BILE) model is employed to accurately impose evolving surface pressure loads throughout the optimization process. The proposed framework integrates the BILE model with a Generalized Optimality Criteria Method (GOCM), offering a robust alternative to the classical Optimality Criteria Method (OCM). GOCM provides greater flexibility in handling constraints and enhances convergence properties. The SIMP-based material interpolation is used, and structural compliance is minimized under a volume constraint using adjoint sensitivity analysis and density filtering. Two benchmark examples are presented to compare the performance of GOCM and OCM under identical DDPL conditions. Quantitative results show that GOCM achieves up to 21.35% lower compliance, reduces computational time by 45.68%, and requires significantly fewer iterations compared to OCM, while maintaining solution quality. These results confirm that GOCM not only improves numerical efficiency but also enhances the stability and effectiveness of topology optimization under complex, evolving load boundaries. The proposed approach offers a reliable and computationally efficient method for advanced structural design problems involving design-dependent loading, with promising applicability in high-performance engineering systems.

Keywords: Topology optimization, design-dependent pressure loading, generalized optimality criteria method, OCM, BILE model
2020 MSC: 74G15, 74P05, 74P10, 74P15, 74P99

1 Introduction

Topology optimization has evolved into a powerful tool for structural design, enabling the optimal distribution of material within a given design space. Since the foundational work by Bendsøe and Kikuchi [2], who introduced the homogenization method for topology optimization, this area of research has undergone substantial developments. Various numerical methods, such as the Solid Isotropic Material with Penalization (SIMP) method [20], Evolutionary Structural Optimization (ESO/BESO) [22], and the Level Set Method [17], have been developed to tackle a broad spectrum of design problems.

*Corresponding author
Email addresses: s.abedini@semnan.ac.ir (Saeed Abedini), aghoddosian@semnan.ac.ir (Ali Ghoddosian)

Received: July 2025 *Accepted:* September 2025

In many practical applications, especially those involving fluidic or surface-contact interfaces, the applied loads are not fixed but depend on the evolving geometry of the structure during optimization. These so-called design-dependent pressure loads (DDPLs) introduce complex challenges, both in terms of load modeling and sensitivity analysis [25]. Unlike fixed loads, DDPLs change location, magnitude, or direction as the boundary of the structure evolves, making traditional approaches inadequate or inefficient.

Several modeling techniques have been proposed to address DDPLs. Chen and Kikuchi [5] introduced the use of fictitious thermal loads to approximate pressure distributions. Hammer and Olhoff [9] modeled pressure through Bézier curves to maintain smoothness across evolving boundaries. Du and Olhoff [6] later enhanced this approach using iterative information from previous optimization steps to improve the accuracy of pressure application.

Bourdin and Chambolle [4] proposed a three-phase material model for better handling of load-structure interaction in DDPL problems. Despite these contributions, no single technique has emerged as a definitive standard, primarily due to the inherent complexity and context-specific behavior of DDPLs. Recent years have seen renewed attention to this challenge. Kumar et al. [15] introduced a method based on Darcy's law to model pressure loading in porous, compliant mechanisms. To further support reproducibility and experimentation, Kumar developed TOPress, a MATLAB code tailored for 2D DDPL problems [13], and subsequently extended it to 3D applications with the release of TOPress3D [14].

New hybrid methods combining structural sub-modeling and experimental validations have also been proposed to improve robustness and physical accuracy [18].

In topology optimization, three main gradient-based algorithms are widely employed due to their efficiency and simplicity: the Optimality Criteria Method (OCM) [7], and the Method of Moving Asymptotes (MMA) [21]. These methods are particularly suited to problems characterized by a large number of design variables—often equal to the number of finite elements in the SIMP approach [27]and relatively few objectives and constraints. Given the high computational cost of finite element analyses at each iteration, their popularity stems from their low computational overhead and avoidance of second-order derivative (Hessian) calculations.

Although gradient-free algorithms such as genetic algorithms [28], particle swarm optimization [8], simulated annealing [19], and Nelder–Mead simplex [26] offer flexibility in handling non-differentiable or discrete design spaces, their requirement for tens of thousands of function evaluations makes them impractical in this context. Thus, gradient-based methods remain the standard despite limitations like sensitivity to local optima and numerical noise.

Among gradient-based methods, adjoint sensitivity analysis [16] outperforms direct differentiation owing to its superior computational efficiency in managing optimization problems characterized by limited objective functions and extensive design parameters. The OCM, popularized through the 99-line MATLAB code [23], is particularly effective for compliance minimization under volume constraints due to its simplicity and low computational cost. However, it lacks generality. In contrast, MMA offers broader applicability by using convex approximations [24] but may be sensitive to algorithmic parameters and computationally expensive for large-scale problems with multiple active constraints. While the substantial progress in load modeling and sensitivity analysis under DDPL conditions, the majority of existing approaches have focused on improving physical fidelity and computational robustness, while less attention has been paid to the impact of optimization algorithm selection on the convergence quality and final topologies.

In this study, we address the topology optimization of structures under compressive design-dependent pressure loads, where the pressure magnitude and direction are functions of the evolving boundary. The load modeling is based on the Boundary Identification–Load Evolution (BILE) model proposed by Ibhadode et al. [11], which enables a consistent and robust representation of DDPLs by tracking the boundary and applying normal surface loads that evolve with the topology. This formulation avoids artificial parameter tuning and guarantees load continuity across iterations, making it suitable for high-resolution optimization tasks.

While previous work using BILE has typically employed the standard Optimality Criteria Method (OCM) for design updates, this paper proposes a novel application of the Generalized Optimality Criteria Method (GOCM), as introduced by Kim et al. [12], to replace OCM in the DDPL-BILE framework. The GOCM reformulates the optimality update using a generalized Lagrangian approach that improves convergence stability and allows for a broader class of constraints and objective functions. Compared to classical OCM, which is limited to problems with explicit volume constraints and compliance objectives, GOCM enables more flexible extensions and better accommodates the numerical complexity induced by design-dependent loading.

The motivation for employing GOCM arises from its ability to balance physical fidelity and numerical robustness. In problems involving DDPLs, the pressure distribution and structural response can be highly sensitive to small changes in topology, which often results in numerical instabilities and oscillatory convergence when using traditional OCM. By incorporating GOCM, this work aims to demonstrate improved convergence behavior and enhanced resolution of fine structural features under pressure-driven loading. The effectiveness of the proposed approach will be validated through numerical examples in subsequent sections.

The remainder of this paper is structured as follows: Section 2 presents the problem formulation under compressive DDPLs using the BILE model. Section 3 introduces the Generalized Optimality Criteria Method. Section 4 provides numerical examples to validate the proposed approach, including two benchmark problems under pressure loading. The final section provides concluding remarks and outlines possible directions for future research.

2 Prbolem Fromulation of DDPL by BILE model

The topology optimization of structures subjected to design-dependent pressure loads presents distinct challenges due to the evolving nature of load magnitudes and directions as the structural topology updates. A robust mathematical formulation and computationally efficient methodology are imperative for accurately characterizing these dynamic responses and ensuring optimal structural performance. This work employs a modified solid isotropic material with penalization (SIMP) framework to establish the problem foundation and introduces the boundary identification-load evolution (BILE) model for the effective tracking of evolving boundaries and application of pressure loads during topology optimization [11].

The optimization problem begins with the consideration of a structural element comprising material and void domains within a fixed design domain Ω, incorporating prescribed boundary conditions and external loading. The design domain is discretized for finite element analysis with fixed degrees of freedom Γ_u, surface loads Γ_t, and volumetric body forces F_b applied (as shown in Figure 1).

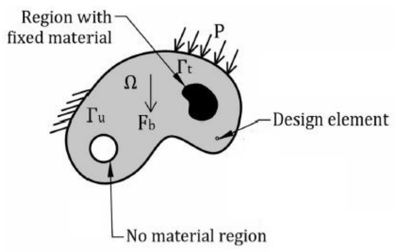

Figure 1: A structural element with load and boundary conditions [11]

The elastic equilibrium state of the structure is expressed by the principle of virtual work, which for an arbitrary virtual displacement v leads to the integral equation [10]:

$$\int_{\Omega} \varepsilon^T(v) D \varepsilon(u)\, d\Omega = \int_{\Omega} F_b^T v\, d\Omega + \int_{\Gamma_t} P^T v\, d\Gamma \tag{2.1}$$

where ε denotes the strain vector, D the material stiffness matrix, u the displacement field, and t the pressure traction applied on boundary Γ_t. The weak form 2.1 can be reformulated in terms of bilinear and linear forms:

$$a(u, v) = l(v), \forall v \in V \tag{2.2}$$

where:

$$a(u, v) = \int_{\Omega} \varepsilon^T(v) D \varepsilon(u)\, d\Omega \tag{2.3}$$

and:

$$l(v) = \int_{\Omega} F_b^T v\, d\Omega + \int_{\Gamma_t} P^T v\, d\Gamma \tag{2.4}$$

The fundamental objective of topology optimization in this context is to minimize the structural compliance, defined equivalently as the strain energy response to applied loads, subject to equilibrium constraints and a volumetric design constraint, formulated within a finite element framework:

$$
\begin{gathered}
\min C = l(u) = F^T U = U^T K U = \sum_{e=1}^{n} E_e(x_e) u_e^T k_0 u_e \\
\text{subject to} : K(x)U(x) = F \\
\sum_{e=1}^{n} V(x_e) \leq f V_0 \\
0 \leq x_e \leq 1 \\
0 \leq E_{min} \leq E_e \leq E_0
\end{gathered}
\tag{2.5}
$$

Here, x_e is the density design variable for element e, $E_e(x_e)$ the interpolated Young's modulus dependent on x_e, k_0 the stiffness matrix of a solid element, $u_e$the element displacement vector, $V(x_e)$the element volume, and fV_0 the allowed volume fraction constraint where f is typically less than unity.

To avoid singularities in the stiffness matrix at intermediate densities, the study adopts the modified SIMP interpolation:

$$
E_e(x_e) = E_{min} + x_e^p (E_0 - E_{min}) \tag{2.6}
$$

where E_{min} represents the small nonzero minimal modulus assigned to void elements, E_0 is the modulus of solid material, and p is the penalization power enhancing binary material distribution. The density $x_e$varies continuously between zero and one, inclusive.

The setup is extended to uniformly distributed surface pressure loads P, recognizing that design-dependent pressure loads alter in location, magnitude, and orientation corresponding with the topology evolution. This necessitates accurate identification of moving boundaries and reapplication of loads at each optimization iteration, a central computational challenge addressed herein.

The BILE model introduces a two-phase approach starting with boundary identification through a volume fraction threshold criterion. Given the density distribution of finite elements, boundary nodes b_n are identified by evaluating the mean density $x_{n,i}$ of all neighboring elements around node n. The threshold volume fraction f_{th} dynamically evolves per iteration as [23]:

$$
f_{th} = f exp^{\left(\frac{it}{\mu} - 1\right)} \tag{2.7}
$$

where it is the current iteration number, μ is a rate-controlling scalar parameter (typically $50 < \mu < 150$), and f is the volume fraction constraint. This exponential progression of f_{th} mirrors the increasing definition and solidity of the topology boundary as optimization matures, bounded by a maximum of 0.8 to prevent premature boundary locking.

The selection of boundary nodes is refined by their adjacency relations based on [11]:

$$
b_n = \begin{cases} 1 & \text{if } x_{sn,l} < f_{th} \text{ for } l = 1, 2 \text{ and } x_{n,i} > 0 \\ 1 & \text{if } x_{n,i} < f_{th} \\ 0 & \text{otherwise} \end{cases} \tag{2.8}
$$

where $x_{sn,l}$ represents the densities surrounding adjacent nodes S_n of node n. This criterion forms a narrow band of boundary nodes dominant at critical density transition zones, facilitating smooth boundary extraction.

Building on this, pressure load application and evolution proceed by selecting loading nodes from these boundary nodes, constrained by their proximity and directional visibility relative to the initial loading surface. The force direction at each loading node is derived from geometric angles formed by the neighboring loading nodes, quantified trigonometrically as [11]:

$$
\begin{gathered}
\Delta\theta_j = \left| \tan^{-1}\left(\frac{\Delta v_j}{\Delta u_j}\right) \right| \\
\theta_j = \begin{cases} \Delta\theta_j & +\Delta u_j,\, +\Delta v_j \\ \pi - \Delta\theta_j & +\Delta u_j,\, -\Delta v_j \\ \pi + \Delta\theta_j & -\Delta u_j,\, -\Delta v_j \\ 2\pi - \Delta\theta_j & -\Delta u_j,\, +\Delta v_j \end{cases}, \quad j = 1, 2, 3, \ldots, n
\end{gathered}
\tag{2.9}
$$

where Δu_j and Δv_j denote the Cartesian coordinate differences between adjacent loading nodes. Subsequently, the equivalent nodal forces representing the pressure load are determined through:

$$F_j = \frac{PA}{N}\left\{\cos(\theta_j)\,u + \sin(\theta_j)\,v\right\} \tag{2.10}$$

with P the applied pressure magnitude, A the surface area or line length under load, N the number of loading nodes, and u,v unit vectors in the horizontal and vertical Cartesian directions, respectively.

The equivalent force magnitudes are approximated to remain constant across iterations to simplify sensitivity calculations, based on mesh fineness and load node congruence. Force directions are updated by comparing mean densities of opposing nodes adjacent to each loading node, which dictates the load evolution or movement.

The load evolution frequency relative to boundary identification is controlled by the parameter n_{le} , defining the number of load evolution iterations between successive boundary identifications. This parameter dynamically decreases as the solution converges, controlling optimization speed and stability (Figure 2 illustrates the workflow). For instance, may start at 7 in early iterations and reduce to 3 in later iterations for efficient convergence [11].

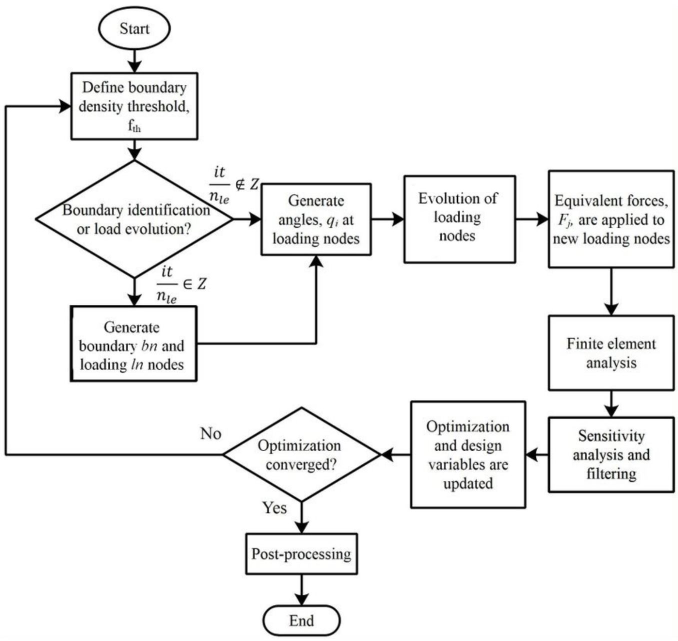

Figure 2: Workflow of the BILE model [11]

Sensitivity analysis is derived via the adjoint method, a rigorous approach to obtain gradients of performance metrics with respect to design variables, fundamental for gradient-based topology optimization. The augmented compliance function including a Lagrange multiplier λ to enforce the equilibrium constraint is [11]:

$$C^* = C(U,x) - \lambda^T(KU - F) \tag{2.11}$$

where $C(U,x) = U^T KU$ is the compliance, K the global stiffness matrix function of design variables x, $U$the displacement vector, and F the load vector. Differentiation with respect to a design variable x_i yields:

$$\frac{\partial C^*}{\partial x_i} = \frac{\partial U^T}{\partial x_i}KU + U^T\frac{\partial K}{\partial x_i}U + U^T K\frac{\partial U}{\partial x_i} - \lambda^T\frac{\partial K}{\partial x_i}U - \lambda^T K\frac{\partial U}{\partial x_i} + \lambda^T\frac{\partial F}{\partial x_i} \tag{2.12}$$

Given the equilibrium condition $KU - F = 0$, the Lagrange multiplier can be suitably set to $\lambda = 2U$ to simplify expression to:

$$\frac{\partial C^*}{\partial x_i} = -U^T\frac{\partial K}{\partial x_i}U + 2U^T\frac{\partial F}{\partial x_i} \tag{2.13}$$

The first term, pertaining to stiffness sensitivity, is straightforward to compute. Notably, the BILE model approximates the load sensitivity term $\frac{\partial F}{\partial x_i}$ as zero based on the principle that equivalent nodal forces' magnitudes remain nearly invariant against the design variables due to the constant pressure assumption over the evolving boundary nodes and small changes in load node count and positions. The forces' angles depend on node locations rather than element densities, significantly reducing computational complexity.

Consequently, the elemental compliance sensitivity simplifies to:

$$\frac{\partial c_e}{\partial x_i} = -u_e^T \frac{\partial K}{\partial x_i} u_e = -p x_i^{p-1} (E_0 - E_{\min})\, u_e^T k_0 u_e \tag{2.14}$$

under the assumption of unit element volume for uniform mesh discretization:

$$\frac{\partial v_e}{\partial x_e} = 1 \tag{2.15}$$

To suppress checkerboarding, mesh-dependency, and numerical instabilities, a sensitivity filtering scheme is employed. It distributes sensitivity contributions from neighboring elements through a length-scale weighted average described by [1]:

$$\frac{\partial \tilde{c}_e}{\partial x_e} = \frac{1}{\max(\gamma, x_e)} \cdot \frac{\sum\limits_{i \in N_e} H_{ei} x_i \dfrac{\partial c_i}{\partial x_i}}{\sum\limits_{i \in N_e} H_{ei}} \tag{2.16}$$

where N_e is the set of neighboring elements within radius r_{min}, $\gamma = 10^{-3}$ a small constant avoiding zero denominator, and H_{ei} defined by:

$$H_{ei} = \max\left(0,\, r_{\min} - d(e,i)\right) \tag{2.17}$$

with $d(e,i)$ measuring the Euclidean distance between element centroids.

3 Generalized optimality criteria method

The conventional Optimality Criteria Method (OCM) has served as a foundational algorithm in topology optimization [3], particularly when coupled with the Solid Isotropic Material with Penalization (SIMP) model. In this framework, the design variables are defined as elemental densities x_e for $e = 1, ..., N_e$. The typical optimization problem can be formulated as:

$$\begin{gathered} \min\, c(x) = \sum_{e=1}^{N_e} x_e^p\, u_e^T k_e u_e \\ \text{subject to: } \frac{V(x)}{V_0} = f \\ K(x)U(x) = F \\ x_{min} \leq x \leq x_{max} \end{gathered} \tag{3.1}$$

where $x = [x_1,\, x_2,\, ...,\, x_{N_e}]^T$, p is the penalization factor (typically 3), k_e and u_e are the elemental stiffness matrix and nodal displacements, respectively, and $V(x) = \sum_{e=1}^{N_e} x_e\, v_e$ denotes the total material volume with v_e as the volume of element e. The compliance function $c(x)$ serves as the objective to be minimized, subject to a volume fraction constraint.

Given the equilibrium condition $KU = F$, sensitivity derivatives of the compliance and volume constraints can be efficiently computed as:

$$\begin{gathered} \frac{\partial c}{\partial x_e} = -p x_e^{p-1}\, u_e^T k_e u_e \\ \frac{\partial V}{\partial x_e} = v_e \end{gathered} \tag{3.2}$$

A Lagrangian function is introduced to handle the constraint using a lagrange multiplier λ:

$$\mathcal{L}(x, \lambda) = c(x) + \lambda\left(V(x) - f V_0\right) \tag{3.3}$$

The Karush–Kuhn–Tucker (KKT) conditions are then expressed as:

$$\frac{\partial \mathcal{L}}{\partial x_e} = \frac{\partial c}{\partial x_e} + \lambda \frac{\partial V}{\partial x_e} = 0, \quad V(x) = f V_0 \tag{3.4}$$

To satisfy the first-order conditions iteratively, the OCM introduces a scale factor D_e for each element:

$$D_e = -\frac{\dfrac{\partial c}{\partial x_e}}{\lambda \dfrac{\partial V}{\partial x_e}} \tag{3.5}$$

The design update is then performed using:

$$x_e^{\text{new}} = \max\left(x_{\min},\ \min\left(x_{\max},\ x_e^{\text{old}}\sqrt{D_e}\right)\right) \tag{3.6}$$

As illustrated in Figure 3, allowable changes to x_e are confined within a move limit $\Delta x_{\max}$, enforcing controlled updates in each iteration.

In the outer loop, the bisection method determines to satisfy the volume constraint. This two-level scheme—an inner loop for x_e, and an outer loop for λ—is effective for single-constraint problems but lacks generalizability to multiple constraints.

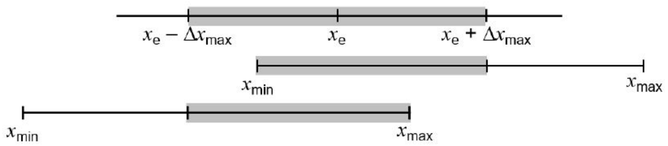

Figure 3: Possible ranges of design change in the optimality criteria [12]

The Generalized Optimality Criteria Method (GOCM) extends the classical OCM to handle problems involving multiple inequality constraints with arbitrary objective functions [12]. The general form of the constrained problem is:

$$\begin{aligned} &\min\ f(x) \\ \text{subject to:}\quad &g_i(x) \le 0, \quad i = 1, \dots, NC \\ &KU = F \\ &x_{\min} \le x \le x_{\max} \end{aligned} \tag{3.7}$$

Here, $g_i(x)$ represents the i^{th} normalized inequality constraint. Using the Lagrangian framework, a generalized Lagrange function is formulated as:

$$\mathcal{L}(x, \lambda, s) = f(x) + \sum_{i=1}^{NC} \lambda_i \left(g_i(x) + s_i^2\right) \tag{3.8}$$

with $\lambda = [\lambda_1,\ \lambda_2,\ \dots,\ \lambda_{NC}]^T$ and slack variables s_i^2 . The KKT stationarity conditions are:

$$\begin{gathered} \nabla f + \sum_{i=1}^{NC} \lambda_i \nabla g_i = 0 \\ g_i(x) + s_i^2 = 0, \quad \lambda_i s_i = 0 \end{gathered} \tag{3.9}$$

Unlike traditional OCM, GOCM avoids strict enforcement of these conditions in every iteration. Instead, Lagrange multipliers are updated progressively, converging only when the optimization stabilizes. To initialize λ_i , a decoupled inverse form is applied:

$$\lambda_i = -\frac{\nabla_x f^T \nabla_x g_i}{\nabla_x g_i^T \nabla_x g_i} \tag{3.10}$$

Subsequently, an adaptive update rule is used:

$$\lambda_i^{k+1} = \lambda_i^k \left[1 + p_0 \left(g_i^k + \Delta g_i^k\right)\right] \tag{3.11}$$

where $\Delta g_i^k = g_i^k - g_i^{k-1}$, and p_0 is a tuning parameter. This update accommodates constraint activation/deactivation over iterations and avoids costly bisection procedures. Design variables are updated using an extended scale factor formulation:

$$D_e = -\frac{\left\langle \frac{\partial f}{\partial x_e} \right\rangle_- + \sum_{i=1}^{NC} \lambda_i \left\langle \frac{\partial g_i}{\partial x_e} \right\rangle_-}{\left\langle \frac{\partial f}{\partial x_e} \right\rangle_+ + \sum_{i=1}^{NC} \lambda_i \left\langle \frac{\partial g_i}{\partial x_e} \right\rangle_+} \tag{3.12}$$

with $\langle a \rangle_+ = \max(0, a)$ and $\langle a \rangle_- = \min(0, a)$. When $D_e = 1$, the stationarity condition is satisfied. This reformulated GOCM enables efficient, stable, and general-purpose topology optimization for problems involving multiple and diverse constraints, overcoming key limitations of the conventional OCM.

4 Numerical examples

This section presents a numerical example to evaluate the impact of employing the Generalized Optimality Criteria Method (GOCM) in topology optimization under design-dependent pressure loads (DDPLs), in comparison to the classical Optimality Criteria Method (OCM).

The design domain is discretized using four-node square elements under plane stress assumptions. The applied pressure load, assumed to have a unit magnitude, acts normal to the evolving boundary at each optimization step. The material properties are defined as follows: Young's modulus of the solid material $E_0 = 1$, Young's modulus of the void $E_{min} = 1 \times 10^{-9}$, and Poisson's ratio $\nu = 0.3$.

To ensure numerical stability and eliminate checkerboarding patterns, a density filter is employed with a radius equal to 2.5 times the element edge length. The optimization process is implemented in MATLAB, and both OCM and GOCM are separately used as optimizers for the same problem setup. The convergence criterion is set to a relative change in element densities of less than 0.015, and the maximum number of iterations is limited to 300. All simulations are performed on a computer equipped with an Intel Core i5 processor 2.4 GHz and 4 GB of RAM.

In both cases, the same boundary conditions, material properties, mesh, and filtering parameters are used to ensure a fair comparison. The differences in resulting topologies, compliance values, and convergence trends are analyzed to illustrate the advantages of the GOCM over the traditional OCM, particularly in dealing with the numerical challenges posed by design-dependent pressure loading.

4.1 Unidirectional externally loaded structures

The design domain illustrated in Figure 4 is a rectangular region with length L and width $\frac{L}{2}$. A pressure load is applied along the top edge, while two fixed boundary conditions are imposed at points located at a distance of $0.1L$ from the bottom corners. The discretization consists of 120 elements along the direction and 60 elements along the direction. The problem was initially solved using the OCM approach, followed by the application of the GOCM method. The corresponding optimization outcomes are depicted in Figure 5 and Figure 6. As observed, the resulting optimal configurations obtained by both methods exhibit similar geometric characteristics. The quantitative numerical results from the optimization procedures are summarized in Table 1. The results reveal that employing the Generalized Optimality Criteria Method (GOCM) leads to a 0.64% reduction in the optimal compliance, an 11.29% decrease in total computational time, and a reduction of 9 iterations compared to the standard Optimality Criteria Method (OCM). These improvements not only reflect a better optimal solution but also indicate enhanced computational efficiency. Furthermore, the convergence behavior observed with GOCM demonstrates superior stability and performance characteristics.

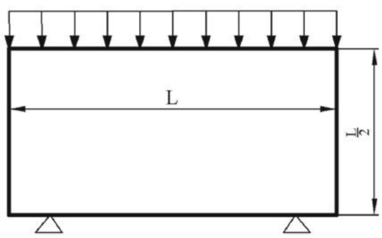

Figure 4: Design domain and boundary condition

Figure 5: Optimum design

Table 1: Comparison of optimum designs using different optimization algorithm

Algorithm	Iteration	Compliance	Volume Fraction	Total Time (s)
OCM	91	25203.442	0.29	124
GOCM	82	25042.852	0.3	110

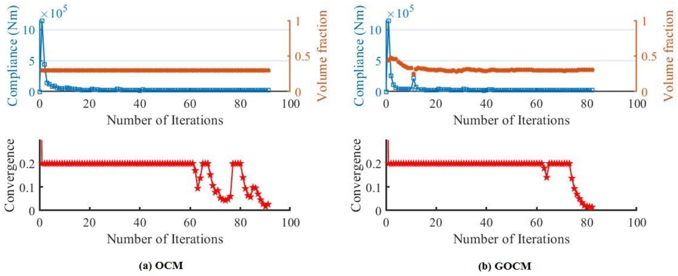

Figure 6: Volume fraction, compliance and convergence

4.2 A beam under pressure loading

Figure 7 illustrates the boundary conditions and loading applied to a beam. The number of elements in the x and y directions is set as in Example 1. The problem is solved separately using the OCM optimizer and subsequently the GOCM. The final optimal designs are presented in Figure 8, while additional optimization results are shown in Figure 9. Moreover, the numerical results obtained from the optimization process are summarized in Table 2.

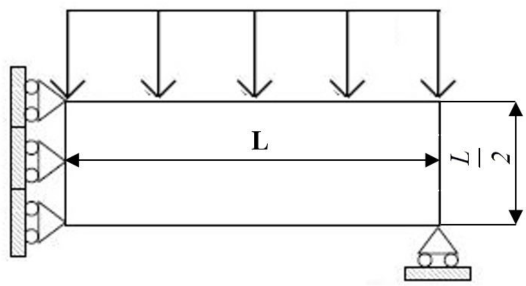

Figure 7: Design domain and boundary condition

Figure 8: Optimum design

Table 2: Comparison of optimum designs using different optimization algorithm

Algorithm	Iteration	Compliance	Volume Fraction	Total Time (s)
OCM	146	577954	0.3	243
GOCM	98	454718	0.3	132

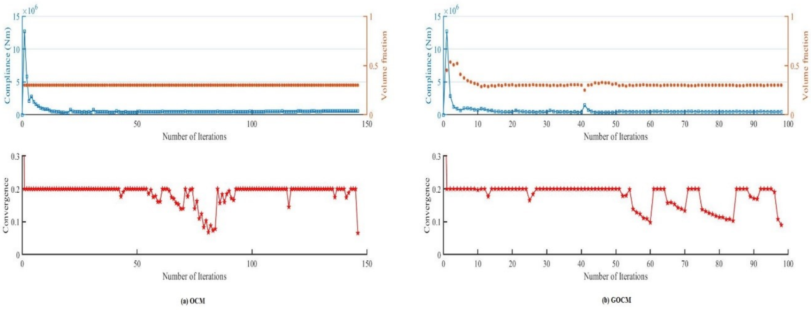

Figure 9: Volume fraction, compliance and convergence

The numerical results confirm that using the Generalized Optimality Criteria Method (GOCM) significantly improves computational efficiency compared to the standard OCM. Specifically, GOCM achieves a 21.35% reduction in the optimal compliance, a 45.68% decrease in total computational time, and requires 48 fewer iterations to reach convergence. These improvements demonstrate the superior performance and robustness of GOCM in solving topology optimization problems under design-dependent pressure loads.

5 Conclution

This study presents a comprehensive topology optimization framework for structures subjected to compressive design-dependent pressure loads (DDPLs), integrating the Boundary Identification–Load Evolution (BILE) model with the Generalized Optimality Criteria Method (GOCM). DDPLs introduce unique challenges due to evolving pressure application points and boundary geometries during iterative design. The BILE model effectively addresses these challenges by consistently applying surface pressure loads throughout the structural evolution, without requiring heuristic modifications or artificial penalization.

Replacing the classical Optimality Criteria Method (OCM) with GOCM, which employs a generalized Lagrangian formulation, provides a more flexible and stable update mechanism, enhancing robustness and convergence, particularly in strongly load-coupled problems. Using SIMP material interpolation, the proposed approach minimizes compliance under a volume constraint via adjoint sensitivity analysis and density filtering.

Numerical case studies demonstrate that GOCM outperforms OCM under identical DDPL conditions, achieving up to 21.35% lower compliance, 45.68% reduction in computational time, and significantly fewer iterations. These results highlight the method's computational efficiency, convergence reliability, and ability to generate high-quality structural layouts.

Despite these achievements, the current study is limited to two-dimensional problems with pressure loads acting normal to evolving boundaries. Extending the framework to three-dimensional domains presents additional theoretical and computational challenges and represents a logical next step for future research. Further developments could include non-normal load orientations, integration with adaptive filtering, uncertainty quantification, and real-time optimization for additive manufacturing applications.

This work establishes a solid foundation for future investigations and provides a rigorous benchmark for applying the BILE–GOCM framework to more complex 3D structural optimization problems under design-dependent pressure loads.

References

[1] E. Andreassen, A. Clausen, M. Schevenels, B.S. Lazarov, and O. Sigmund, *Efficient topology optimization in MATLAB using 88 lines of code*, Struct. Multidiscip. Optim. **43** (2011), no. 1, 1–16.

[2] M.P. Bendsøe and N. Kikuchi, *Generating optimal topologies in structural design using a homogenization method*, Comput. Meth. Appl. Mech. Engin. **71** (1988), no. 2, 197–224.

[3] M. P. Bendsøe and O. Sigmund, *Optimization of Structural Topology, Shape, and Material*, 2nd ed., Springer, Berlin, March 2004.

[4] B. Bourdin and A. Chambolle, *Design-dependent loads in topology optimization*, ESAIM: Control Optim. Cal. Var. **9** (2003), 19–48.

[5] B.C. Chen and N. Kikuchi, *Topology optimization with design-dependent loads*, Finite Elements Anal. Design **37** (2001), no. 1, 57–70.

[6] J. Du and N. Olhoff, *Topological optimization of continuum structures with design-dependent surface loading—Part II: Algorithm and examples for 3D problems*, Struct. Multidiscipl. Optim. **27** (2004), no. 3, 166-177.

[7] W. Fan, Z. Xu, and Z. Zhang, *A PID-optimality criteria method for structural topology optimization*, Optim. Engin. **25** (2024), 439–458.

[8] J. Guan and W. Zhang, *Improved topological optimization method based on particle swarm optimization algorithm*, IEEE Access **10** (2022), 52067–52074.

[9] V.B. Hammer and N. Olhoff, *Topology optimization of continuum structures subjected to pressure loading*, Struct. Multidiscipl. Optim. **19** (2000), no. 2, 85–92.

[10] B. Hassani and E. Hinton, *Homogenization and Structural Topology Optimization*, 1st ed., Engineering Sciences Library, vol. 1, Springer, Berlin, January 1999.

[11] O. Ibhadode, Z. Zhang, P. Rahnama, A. Bonakdar, and E. Toyserkani, *Topology optimization of structures under design-dependent pressure loads by a boundary identification-load evolution (BILE) model*, Struct. Multidiscipl. Optim. **62** (2020), no. 6, 1865–1883.

[12] N. H. Kim, T. Dong, D. Weinberg, and J. Dalidd, *Generalized Optimality Criteria Method for Topology Optimization*, Appl. Sci. **11** (2021), no. 7, 3175.

[13] P. Kumar, *TOPress: A MATLAB implementation for topology optimization of structures subjected to design-dependent pressure loads*, Struct. Multidiscipl. Optim. **66** (2023), no. 4, Article 97.

[14] P. Kumar, *TOPress3D: 3D topology optimization with design-dependent pressure loads in MATLAB*, Optim. Engin. **26** (2025), 1113–1141.

[15] P. Kumar, J.S. Frouws, and M. Langelaar, *Topology optimization of fluidic pressure-loaded structures and compliant mechanisms using the Darcy method*, Struct. Multidiscipl. Optim. **61** (2020), no. 4, 1637–1655.

[16] S. Li, J. Yin, X. Jiang, Y. Zhang, and H. Wang, *A novel reduced basis method for adjoint sensitivity analysis of dynamic topology optimization*, Engin. Anal. Boundary Elements **162** (2024), 403–419.

[17] H. Lin, H. Liu, and P. Wei, *A parallel parameterized level set topology optimization framework for large-scale structures with unstructured meshes*, Comput. Meth. Appl. Mech. Engin. **397** (2022), 115112.

[18] Y. Lu, Q. Luo, and L. Tong, *Topology optimization for pressurized nonlinear structures using substructure and experimental studies*, Struct. Multidiscipl. Optim. **68** (2025), no. 1, Article 31.

[19] H.R. Najafabadi, T.C. Martins, M.S.G. Tsuzuki, and A. Barari, *Structural design with self-weight and inertial loading using simulated annealing for non-gradient topology optimization*, Machines **12** (2024), no. 1, Article 25.

[20] I.P.A. Papadopoulos, *Numerical analysis of the SIMP model for the topology optimization problem of minimizing compliance in linear elasticity*, Numer. Math. **157** (2025), 213–248.

[21] T. Rochefort-Beaudoin, A. Vadean, J. Gamache, and S. Achiche, *Comparative study of first-order moving asymptotes optimizers for the moving morphable components topology optimization framework*, Proc. ASME 2022 Int. Design Engineering Technical Conf. and Computers and Information in Engineering Conf., Vol. 2: 42nd Computers

and Information in Engineering Conference (CIE), St. Louis, Missouri, USA, August 14–17, 2022, V002T02A028, ASME.

[22] S. Sanfui and D. Sharma, *Soft- and Hard-Kill Hybrid Graphics Processing Unit-Based Bidirectional Evolutionary Structural Optimization*, ASME. J. Comput. Inf. Sci. Eng. **24** (2024), no. 4, 041007.

[23] O. Sigmund, *A 99 line topology optimization code written in MATLAB*, Struct. Multidiscipl. Optim. **21** (2001), no. 2, 120–127.

[24] K. Svanberg, *The method of moving asymptotes—a new method for structural optimization*, Int. J. Numer. Meth. Engin. **24** (1987), no. 2, 359–373.

[25] E. Urso, S. Eddine Zerrouq, and M. Montemurro, *A topology optimization method for problems with design-dependent loads based on non-uniform rational basis spline entities*, Mech. Adv. Mater. Struct. **31** (2023), no. 28, 10671–10686.

[26] H. Wu, Y. Chen, Z. Cai, and G. Liang, *Dual-weight decay mechanism and Nelder-Mead simplex boosted RIME algorithm for optimal power flow*, J. Big Data **11** (2024), no. 1, Article 172.

[27] S. Xu, J. Liu, B. Zou, Q. Li, and Y. Ma, *Stress constrained multi-material topology optimization with the ordered SIMP method*, Comput. Meth. Appl. Mech. Engin. **373** (2021), 113453.

[28] J. Zhang and J. Yanagimoto, *Density-based topology optimization integrated with genetic algorithm for optimizing formability and bending stiffness of 3D printed CFRP core sandwich sheets*, Comp. Part B: Engin. **225** (2021), Article 109248.